Journal of
Materials Chemistry B

Materials for biology and medicine

rsc.li/materials-b

Volume 6
Number 3
21 January 2018
Pages 341-528

ISSN 2050-750X

ROYAL SOCIETY
OF CHEMISTRY

PAPER
Wei Wei, Guanghui Ma et al
Macrophage responses to the physical burden of cell-sized
particles

This is an Accepted Manuscript, which has been through the Royal Society of Chemistry peer review process and has been accepted for publication.

Accepted Manuscripts are published online shortly after acceptance, before technical editing, formatting and proof reading. Using this free service, authors can make their results available to the community, in citable form, before we publish the edited article. We will replace this Accepted Manuscript with the edited and formatted Advance Article as soon as it is available.

You can find more information about Accepted Manuscripts in the Information for Authors.

ROYAL SOCIETY
OF CHEMISTRY

rsc.li/materials-b

ARTICLE

A novel mitochondria-targeted ratiometric fluorescent probe for endogenous sulfur dioxide derivatives as a cancer-detecting tool

Di Yang,[‡][a] Xiao-Ying He,[‡][b] Xiao-Tian Wu,[a] Hao-Nan Shi,[a] Jun-Ying Miao,[b] Bao-Xiang Zhao,[a*] Zhao-Min Lin[c*]

A new mitochondria-targeted fluorescence probe RBC, constructed by a coumarin moiety which was selected as the donor and a benzothiazole derivative as the acceptor, for SO_2 derivatives (HSO_3^-/ SO_3^{2-}) was presented. The probe designed on a new FRET platform showed high selectivity and low detection limit. Importantly, the probe could respond to HSO_3^-/ SO_3^{2-} within 35s. Furthermore, the probe could target mitochondria and was successfully used for fluorescence imaging of endogenous bisulfite in HepG2 with low cytotoxicity, which had a significantly assist to cancer diagnosis.

Introduction,

Sulfur dioxide (SO_2) frequently produced by coal and oil[1,2] is the main air pollutant and component of acid rain in many developing countries. Abnormal SO_2 level can cause breathing problems and other health problems such as lung cancer.[3-5] Meanwhile, SO_2 was recognized as a new gasotransmitter because it could be associated with physiological processes and could be produced enzymatically in cytosols and mitochondria of cells.[6] What's more, the detection and quantification of SO_2 is critical in food and environmental monitoring field.[7] Nonetheless, the biological roles of SO_2 still remain largely unknown. SO_2 is easily soluble in water and then can produce two derivatives in aqueous solution, i.e. bisulfite (HSO_3^-) and sulfite (SO_3^{2-}) in 1:3 ratio. So the physiological functions of SO_2 can be attributed to its derivatives. Nowadays a lot of analytical methods such as spectrophotometry, chromatography and electrochemical methods were invented.[8,9] However, the effect is not ideal by reason of handling complexity and low sensitivity, especially, the methods mentioned above cannot achieve real-time imaging in living cells. Therefore, the detection of SO_2 in cells is still a bottleneck problem.

Due to high sensitivity, excellent selectivity, real-time assay, great temporal and spatial sampling capability, fluorescent probe was born at the right time.[10-13] In recent years, a few favorable redox-responsive fluorescent probes have been developed and applied to explore the generation, transport, physiological function, and pathogenic mechanisms of reactive oxygen species and antioxidants.[14] However, most of the probes based on fluorescence intensity may be influenced by many environmental effects.[15] To overcome this drawback, ratiometric fluorescence probe, which can eliminate environmental effects by affording simultaneous ratio signals of two emission intensities at two different wavelengths, is popular nowadays. To date, a few well-behaved ratiometric fluorescence probes for SO_3^{2-}/ HSO_3^- have been developed.[16-20] Even so, some performances such as response time, excitation wavelength and detection limit still remain a big room to improve.[21-23]

Forster resonance energy transfer (FRET), which is the interaction between two fluorophores linked by a non-conjugated spacer in the same molecule, is a new way to construct well-behaved ratiometric probes. FRET is non-radiative energy transfer from an excited dye donor to a dye acceptor in the ground state, which may take place in the dyad to prevent the donor fluorescence and to enhance the acceptor fluorescence.[24] As a consequence, a substantial overlap of the donor emission spectrum with the acceptor absorption is crucial.[25] What's more, the FRET system can rule out the influence of excitation backscattering because of the large pseudo-Stokes shift between donor excitation and acceptor emission and two well-separated emission bands with comparable intensities can ensure detection accuracy. Besides, other factor such as high photo-stability, high quantum yield, good solubility in aqueous and lipid environments, good cell permeability, and low interference from biological environments should be considered when a new probe was designed. Numerous of ratiometric fluorophores were chosen for constructing probes such as hemicyanine,[26] BODIPY,[27] triphenylamine,[28] rhodamine,[29] 1,8-naphthalimide.[30] Coumarin dyes were applied in the design of ratiomatric fluorescent probes because they showed high quantum yield and appropriate water solubility, as well as the low cell toxicity.[31]

Nowadays, benzothiazole derivatives are crucial reagents in pharmaceutical chemistry and have been extensively studied in

[a.] Institute of Organic Chemistry, School of Chemistry and Chemical Engineering, Shandong University, Jinan 250100, P.R. China. E-mail: bxzhao@sdu.edu.cn (B.X. Zhao).

[b.] Institute of Developmental Biology, School of Life Science, Shandong University, Qingdao 266237, P.R. China..

[c.] Institute of Medical Science, the Second Hospital of Shandong University, Jinan 250033, P.R. China. E-mail: linzhaomin@sdu.edu.cn

‡ Equal contribution.

Electronic Supplementary Information (ESI) available: [details of any supplementary information available should be included here]. See DOI: 10.1039/x0xx00000x

the molecular design and biological activity. Benzothiazole derivatives have good biological activity such as antibacterial activity,[32] antitumor activity,[33] and can be used as insecticide[34] and antibacterial agent.[35] In addition, as an electron acceptor, benzothiazole had interesting optical physical properties when it was modified with substituent to form a D-π-A structure. But due to the lack of common synthetic methods, it is of great challenge and fundamental importance to develop an efficient strategy for those compounds.[36,37] Previously, our group designed a new fluorescence ratiometric probe for the detection of reactive oxygen species using benzothiazole as a receptor.[38] Ge's group synthesized another probe to detect HSO_3^- by changing the donor, which exhibited good optical properties,[39] however, the long response time and the low energy transfer efficiency may block the application of this probe.

Herein a new ratiometric fluorescence sensing probe based on FRET is constructed as an alternative for in situ analysis of SO_3^{2-}/HSO_3^- and biological image in cells. A coumarin fluorophore was used as the donor and the (*E*)-3-ethyl-2-(2-methoxystyryl)-2,3-dihydrobenzothiazole was selected as the acceptor on account of well overlap between the coumarin emission and the benzothiazole derivative absorption. The spectroscopic properties showed that probe RBC possessed fast response time and excellent sensitivity. Most important of all, probe RBC showed outstanding real-time image in cells.

Experimental

2.1 Apparatus

^1H NMR (300 MHz) and ^{13}C NMR (75 MHz) spectra were recorded on a Bruker Avance with DMSO-d_6 used as solvent and tetramethylsilane (TMS) as an internal standard. Thin-layer chromatography (TLC) was conducted on silica gel 60F$_{254}$ plates (Merck KGaA) and column chromatography was conducted over silica gel (mesh 200-300). Melting points were determined on an XD-4 digital micro melting point apparatus. High-resolution mass spectrometry (HRMS) was obtained on a Q-TOF6510 spectrograph (Agilent). Fluorescence measurements were recorded on a Perkin-Elmer LS-55 luminescence spectrophotometer. The pH was measured by use of a pHS-3C digital pH-meter (YouKe, Shanghai). Twice-distilled water was used throughout all experiments. All reagents and solvents were purchased from commercial sources and used without further purification.

2.2 Synthesis of probe RBC

Synthesis route of probe RBC is depicted in Scheme S1 and the structure was characterized by ^1H NMR, ^{13}C NMR and HRMS (Fig. S1-S3, ESI).

2.2.1 *Synthesis of Compound 1 and 2*

Compound **1** was synthesized based on the reported method.[40] 2-Methylbenzothiazole (1.49 g) and iodoethane (2.34 g) were dissolved in ethanol (15 mL). The mixture reacted under the condition of refluxing and stirring for about 3 h. After completion of the reaction (monitored by TLC), the reaction mixture was cooled to room temperature, and white solid

precipitated. Then the crude product was purified by recrystallization from mixture solvent (dichloromethane: methanol = 10: 1, v/v) to give compound **1** in 83% yield, m. p.: 193-194 °C.

4-Fluoro-2-methoxybenzaldehyde (3.8 g, 20 mmol) and piperazine (6.479 g, 75 mmol) was dissolved in ethylene glycol monomethyl ether (7 mL) and water (4 mL). The reaction mixture was refluxed and stirred. With the reaction processing, color of the solution gradually deepened and the solution turned dark brown yellow when the reaction finished (monitored by TLC). After cooling to room temperature, water (30 mL) was added into the mixture. The solution was extracted three times with dichloromethane (50 mL×3) and organic phase was washed by saturated brine (200 mL×3). Then organic phase was dried with anhydrous magnesium sulfate overnight. After filtrated, the solvent was removed under reduced pressure to get light brown product. Subsequently, a crude product was purified by flash column chromatography (dichloromethane: methanol = 10: 1, v/v) to obtain compound **2** with 74% yield, m. p.: 186-187 °C.

2.2.2 *Synthesis of Compound 3*

Compound **1** (3.06 g) and compound **2** (2.2 g) were dissolved in ethanol (15 mL) and catalytic amount piperidine was added to the mixture. The reaction mixture was stirred and heated to reflux for about 6 h (monitored by TLC). The solvent was removed under reduced pressure. Subsequently, the crude product was subjected to column chromatography using silica gel as the stationary phase and pure methanol as the mobile phase to obtain unmixed dark orange compound **3** with a yield of 60%, m. p.: 236-237 °C.

2.2.3 *Synthesis of probe RBC*

Compound **3** (292 mg, 0.816 mmol) was dissolved in dry CH_2Cl_2 (20 mL), followed by addition of Et_3N (2 mL) in ice bath for 30 min. Coumarin chloride (200 mg, 0.741 mmol) was added in batches and the reaction solution was stirred under ice bath until the reaction finished (monitored by TLC). The solvent was removed under reduced pressure. The crude solid was purified by column chromatography on silica gel using CH_2Cl_2/CH_3OH (200: 1, v/v) to give bright orange red probe RBC with 65% yield. The melting point of RBC is 190.5-192 °C. ^1H NMR (300 MHz, DMSO-d_6) δ 8.260 (d, J = 7.2 Hz, 1H), 8.198-8.138 (m, 2H), 8.038-8.008 (m, 2H), 7.762 (t, J = 7.5 Hz 1H), 7.708-7.658 (m, 2H), 7.511 (d, J = 9 Hz, 1H), 6.791-6.738 (m, 2H), 6.585-6.551 (m, 2H), 3.392 (s, 3H), 3.745-3.434 (m, 12H), 1.403 (t, J = 7.2 Hz, 3H), 1.116 (t, J = 7.2 Hz, 6H). ^{13}C NMR (75 MHz, DMSO-d_6): 171.67, 164.81, 161.94, 158.99, 157.20, 156.01, 144.83, 144.45, 141,42, 130.71, 129.52, 127.95, 127.54, 124.50, 116.20, 116.02, 112.98, 109.95, 107.90, 107.61, 106.59, 96.76, 96.35, 63.45, 56.58, 44.67, 43.99, 14.18, 12.79; HRMS: m/z calcd for $[C_{36}H_{39}N_4O_4S^+]$ 623.2687, found 623.2564

2.3 Preparation for UV-vis absorption and fluorescence spectrum measurements

Probe RBC was dissolved in DMF to afford the stock solution (1×10^{-3} M). Anions including F$^-$, Cl$^-$, Br$^-$, I$^-$, AcO$^-$, ClO$_3^-$, HCO$_3^-$, SCN$^-$, S$_2$O$_3^{2-}$, HS$^-$, NO$_2^-$, IO$_3^-$, SO$_4^{2-}$, ClO$^-$, HPO$_4^-$, CO$_3^{2-}$, NO$_3^-$, SO$_3^{2-}$, HSO$_3^-$ and active small biological molecules including

cysteine (Cys), homocysteine (Hcy) and glutathione (GSH) were dissolved in twice-distilled water at a concentration of 1×10^{-2} M for the absorption and fluorescence spectrum analysis.
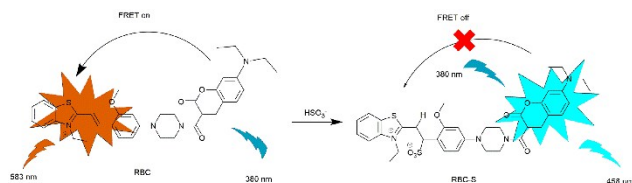
Scheme 1 A proposed recognition mechanism of the probe toward HSO_3^-; Inset: A visual fluorescence change photograph (a) under visible light (b) under illumination using a 365 nm UV lamp.

Test solutions were prepared by placing 100 µL of the stock solution and an appropriate aliquot of each testing species solution into a 10 mL volumetric flask, and the solution was diluted to 10 mL with PBS buffer solution (10 mM, pH = 7.38) containing 30% DMF (v/v). For all measurements of fluorescence spectrum, excitation wavelength was 380 nm, slit width was 15.0/9.0 nm.

2.4 Cell culture and cell imaging

Hela cells were cultured in Dulbecco's modified Eagle's medium (DMEM) (with 10% fetal bovine serum) in a humidified atmosphere of 5% CO_2 and 95% air at 2×10^4 cells per well under 37 °C. Then HeLa cells were pre-incubated with RBC (1 µM) for 1 h, followed by NaHSO$_3$ (0, 20, 100, 500, 750 µM) for another 1 h, and then washed 3 times with PBS buffer. The cells were imaged under a confocal microscope (LSM 700), and the images were collected at emission channels of 450-610 nm (blue channel) and 610-700 nm (red channel) at 405 nm excitation.

HepG2 cells were cultured in Dulbecco's modified Eagle's medium (DMEM, Gibco) supplemented with 10% (v/v) calf bovine serum (HyClone, USA) in an atmosphere of 5% CO_2 and 95% air at 37 °C. HepG2 cells were incubated with RBC (2 µM) for 30 min, and then treated with a mixture of GSH (500 µM) and $Na_2S_2O_3$ (250 µM) for 1 h. HepG2 cells were pretreated with TNBS (10 mM) for 0.5 h, and a mixture of GSH (500 µM) and $Na_2S_2O_3$ (250 µM) was added and cultured for another 0.5 h, then RBC (2 µM) was added and incubated for 1 h. After cells were washed with PBS, cell images were observed with a confocal microscope (Zeiss LSM700) at 405 nm excitation. The emission range of the blue channel was 450-610 nm and the red channel was 610-700 nm.

2.5 Cytotoxicity assay

The cytotoxicity of RBC was evaluated in HeLa cells by a sulforhodamine B (SRB) assay. HeLa cells were cultivated with Dulbecco's modified Eagle's medium (DMEM) which contains supplement of 10% FBS (Fetal Bovine Serum) in the carbon dioxide incubator with an atmosphere of 5% CO_2 and 95% air at 37 °C. HeLa cells were placed to a 96-well plate in the concentration of 40,000 per mL for 24 h, and then incubated with probe RBC (0, 0.1, 1, 5, 10 µM) for 6 h, respectively. After that SRB assay was conducted to measure the viability of cells.

Results and discussion,

3.1 Design and synthesis of the probe (RBC)

Probe RBC based on the reaction of double bond with HSO_3^- was facilely synthesized from coumarin chloride which was selected as donor and (*E*)-3-ethyl-2-(2-methoxystyryl)-2,3-dihydrobenzothiazole as the acceptor by four steps (Scheme S1) and fully characterized by ^{1}H NMR, ^{13}C NMR and HRMS.

As shown in Scheme 1, the probe had the strong emission of the acceptor moiety at 583 nm with the excitation at 380 nm, which exhibited a significant overlap of coumarin emission with benzothiazole derivative absorption and FRET process occurred. However, the FRET process was off when the probe reacted with HSO_3^- affording a nucleophilic addition product RBC-S in which an acceptor fluorophore lacked due to the break of the conjugate system. As the result, the dyad displayed coumarin emission at 458 nm and the color of the probe solution changed from red to light yellow under visible light.

3.2 Property of probe RBC and RBC-S

All the samples were investigated in PBS (0.01 M, pH = 7.38) contained 30% DMF buffer solution. The specific nature of probe RBC was first investigated by UV-vis absorption in the buffer solution. The absorption spectra of free probe RBC in PBS solution exhibited two peaks at 418 nm and 508 nm, which were assigned to the characteristic absorption of coumarin moiety and the acceptor moiety respectively (Fig. S4a).

Also, the fluorescence emission was examined. The free probe exhibited weak coumarin fluorescence at 456 nm and strong acceptor moiety emission at 583 nm (Fig. S4b). The distinct gap between the two emissions is over 127 nm, which means that the probe is favorable for the dual emission ratiometric imaging. Upon addition of enough NaHSO$_3$ to the solution, a significant fluorescence intensity at 583 nm decreased and fluorescence at 456 nm increased with 380 nm excitation (Fig. S5). The red-color solution of RBC became light yellow under visible light, correspondingly, the dark orange fluorescence changed into green under 365 nm UV- irradiation (Fig. S6).

To obtain further insights into the sensitivity of probe RBC for NaHSO$_3$, the fluorescence titration curve (Fig. 1a) and UV-Vis titration curve (Fig. S7) were obtained upon gradual addition of NaHSO$_3$ (0-6 equiv.) to the buffered solution of probe RBC. A 30-fold enhancement of the fluorescence ratio I_{456}/I_{583} was observed when about 6 equiv. NaHSO$_3$ was added. $\ln(I_{456}/I_{583})$ was linearly proportional to the concentrations of NaHSO$_3$ and the $R^2 = 0.993$ illustrated an exact linear relationship (Fig. 1b).
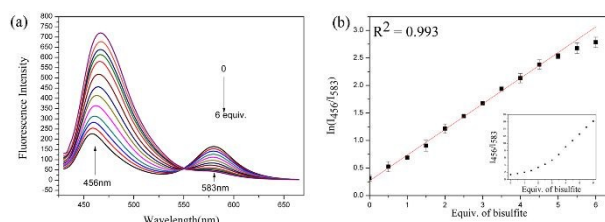
Fig. 1 (a) Fluorescence spectra of the probe (5 µM) with the addition of NaHSO$_3$ (0 up to 6 equiv.) in PBS buffer (pH 7.38, 10 mM, content 30% DMF v: v): (λ_{ex} = 380 nm, slit: 15 nm/9 nm). (b) The linear relationship between $\ln(I_{456}/I_{583})$ and concentration of NaHSO$_3$ (0-6 equiv.). Inset: Ratio (I_{456}/I_{583}) changes upon addition of NaHSO$_3$ (0-6 equiv.) in PBS (pH = 7.38, 10 mM, containing 30% DMF). (RBC = 5 µM), λ_{ex} = 380 nm, slit: 15 nm/9 nm.

ARTICLE
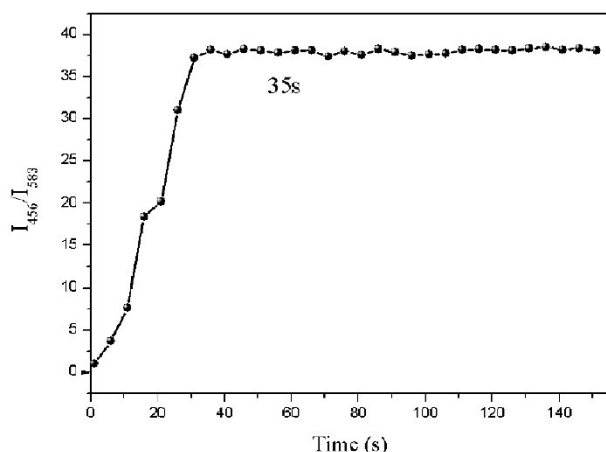
Fig. 2 Time-dependent fluorescence changes of RBC (5 μM) in the presence of bisulfite (6 equiv.). All data were acquired in PBS (pH = 7.38, 10 mM, containing 30% DMF). λex = 380 nm, slits: 15 nm/9 nm.

To shed light on the reaction mechanism, the addition reaction between RBC and HSO_3^- was verified by HRMS data, in which a new peak appeared at m/z 727.2246 was attributed to the addition product (Fig. S8). To further evidence the FRET mechanism, two compounds, free donor (compound **5**) and free acceptor (compound **4**) were synthesized (Scheme S2) and the reactivity toward HSO_3^-/SO_3^{2-} was examined. Comparing the fluorescence and absorption intensities of the donor (compound **5**) and the acceptor (compound **4**) upon addition of NaHSO3 (6 equiv.), the fluorescence of compound **5** was quenched whereas that compound **4** was unaffected (Fig. S9). What' more, the absorption band peaked at 508 nm was decreased dramatically and the band peaked at 418 nm nearly did not change. It suggested that the acceptor moiety of RBC interacted with NaHSO₃ while the coumarin moiety did not. Notably, the fluorescence emission wavelength of the donor (compound **5**) had a significantly overlaps with the absorption of the acceptor (compound **4**) (Fig. S10). The energy transfer efficiency of probe RBC was calculated to be 95%. So for probe RBC, the FRET process occurred effectively from the donor fluorophore to the acceptor fluorophore once the donor was excited. What's more, the probe and donor (compound **4**) both can be excited at 380 nm, however, the acceptor (compound **5**) cannot, which further confirmed the FRET process in probe RBC.

3.3 Selectivity and sensitivity of probe RBC

The selectivity of RBC toward HSO_3^-/SO_3^{2-} over various biological relevant anions (F^-, Cl^-, Br^-, I^-, AcO^-, ClO_3^-, HCO_3^-, SCN^-, $S_2O_3^{2-}$, HS^-, NO_2^-, IO_3^-, SO_4^{2-}, $HClO$, HPO_4^-, CO_3^{2-}, NO_3^-, SO_3^{2-}, HSO_3^-) and small molecules (Cys, Hcy, GSH) was investigated (Fig. S11 - S12). Addition of these representative interfering species induced no apparent ratio increase. Only HSO_3^- and SO_3^{2-} led to a big enhancement ratio. It suggested that RBC had a strong ability to resist interference and was able to detect HSO_3^-/SO_3^{2-} without any distinct interference from other anions. The absorption spectrum of RBC toward bisulfite and various competitive species showed also outstanding selectivity.

3.4 The detection limit of RBC toward HSO_3^-

The limit of detection (LOD) and limit of quantitation (LOQ) are calculated according to the equations (ESI),[10] where σ is the standard deviation of the blank and S is the absolute magnitude of the calibration curve's slope, respectively. The LOD and LOQ were 0.0126 μM and 0.0379 μM, which is superior to previous reports (Table S1). The satisfactory sensitivity is potential for the detection of intracellular SO_2 derivatives.

3.5 pH effect and response time

To evaluate the effect of pH on the sensing HSO_3^-, we studied the fluorescence spectra of RBC in the range of pH 3 to 10 (Fig. S13). Probe RBC itself is stable at a pH range of 3-10, revealing the stability of the probe at physiological pH conditions. After addition of HSO_3^- to the buffer solution, the maximal emission intensity ratio enhanced obviously compared with free probe and was still stable at basicity condition, suggesting that the probe could sense properly HSO_3^- at physiological pH, which is more suitable for application in mitochondria. We chose pH value of 7.38 (buffer solution) in this work.

Subsequently, time-dependent fluorescence response of RBC toward NaHSO₃ was investigated. To our surprised, the probe reached a maximum plateau within 35s toward HSO_3^-, and I_{456}/I_{583} peaked and remained unchanged in 30 min. Such a rapid response is faster than most of reported probes, which is appealing to real-time in vivo imaging (Fig. 2).

3.6 Fluorescence quantum yield

The fluorescence quantum yield of RBC in PBS (contain 30% DMF) was 3%.

3.7 Cell image

Encouraged by the above results, the application performance of probe RBC in living cells was explored.

Cytotoxicity and photo-stability of RBC were primarily evaluated. The SRB assay in living Hela cells showed that the viability of cells had inconspicuous variation after treated with probe RBC (0.1, 1, 5, 10 μM) for 6 h (n = 3) which indicated that the probe had no obvious cytotoxicity in Hela cells. As a result, probe RBC may be applicable in living cells with minimum interference (Fig. S14). From the control fluorescence images of Hela cells incubated with probe RBC (1 μM) for continuously irradiating different times, we found that the red and blue fluorescence had no apparent change, which exhibited excellent photo stability in Hela cells, meaning the feasibility of
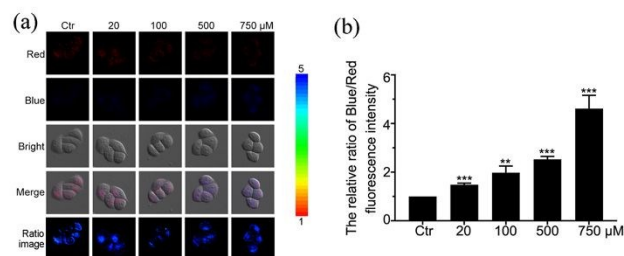
Fig. 3 (a) Fluorescence and bright field images and (b) the ratio of fluorescence intensity (blue/red) of HeLa cells incubated with probe RBC (1 μM) for 1 h and then with NaHSO₃ (0, 20, 100, 500 and 750 μM) for 1 h. The ratio images were all obtained as F_{blue}/F_{red}, $λ_{ex}$ = 405 nm; $λ_{em}$ = 450–610 nm (blue), $λ_{em}$ = 640–700 nm (red). **P < 0.01; ***p<0.001 (n = 3).

Journal Name

ARTICLE
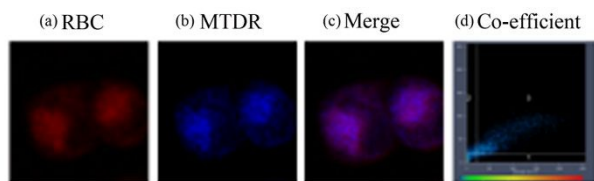
Fig. 4 HeLa cells were incubated with RBC (3 µM) for 1 h, followed by Mito Tracker Deep Red (1 µM) for 20 min. (a) The fluorescence image of RBC. λ_{ex} = 405 nm, λ_{em} = 450–610 nm. (b) The fluorescence image of Mito Tracker Deep Red. λ_{ex} = 639 nm, λ_{em} = 640–700 nm. (c) Merged images of (a) and (b). (d) Colocalization coefficient (Pearson's coefficient) of RBC and Mito Tracker Deep Red was 0.93.
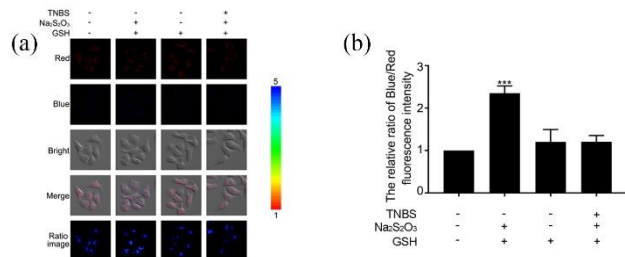
Fig. 5 Image of endogenous bisulfite in HepG2 cells. (a) Fluorescence, bright field and ratio images. HepG2 cells were pre-incubated with RBC (2 µM) for 1 h, then with GSH (500 µM)/ $Na_2S_2O_3$ (250 µM) or GSH (500 µM) for another 0.5 h. Otherwise, RBC loaded HepG2 cells were pre-incubated with TNBS (10 mM) for 0.5 h, then with GSH (500 µM)/ $Na_2S_2O_3$ (250 µM) for another 0.5 h. (b) The relative ratio of blue/red fluorescence intensity of probe RBC alone (column 1), and in the presence of GSH/ $Na_2S_2O_3$ (column 2), GSH (column 3), TNBS/GSH/$Na_2S_2O_3$ (column 4). The ratio images were all obtained as F_{blue}/F_{red}. Images were acquired from 450 to 610 nm for blue fluorescence, and from 610 to 700 nm for red fluorescence. λ_{ex} = 405 nm.

performing cell image assays by using confocal microscopy (Fig. S15).

Further, the detection of intracellular HSO_3^- in living Hela cells was studied. Hela cells were incubated with RBC (1 µM) for 1 h, strong fluorescence in the red channel and weak fluorescence in the blue channel were observed, which showed that the probe managed great cell membrane permeability (Fig. 3). However, when cells were incubated with different concentrations of HSO_3^-, a dramatical improvement of the emission ratio (blue/red) in the stained cells, with a remarkable deepening in blue channel and decline of red channel fluorescence was observed (Fig. 3). The results manifested probe RBC could effectively detect exogenous HSO_3^-.

The distribution of the probe in organelles was explored. The Mito Tracker Deep Red, a kind of commercial dye, can be accumulated in mitochondria. The colocalization assay with probe RBC and Mito Tracker Deep Red manifested that probe RBC distributed mainly in the mitochondria (Quantitation of co-localization coefficients: 0.93) (Fig. 4).

It is well known that endogenous bisulfite is produced by the decomposition thiosulfate which generated from the reaction of GSH with $Na_2S_2O_3$ via TST (thiosulfate sulfurtransferase enzyme) that is widely distributed in mammalian liver cells. Therewith HepG2 cells were chosen for detecting endogenous bisulfite. After HepG2 cells were incubated with the probe, followed by incubation with GSH and $Na_2S_2O_3$, evident

fluorescence changes were observed because of the production of endogenous bisulfite (Fig. 5). However, there was no significant variation when the cells were only incubated with the probe and GSH, because there was no condition to form bisulfite. Moreover, still no significant fluorescence change was observed when the HepG2 cells were pre-treated with 10 mM TNBS (2, 4, 6-trinitrobenzenesulphonate) which is known as a TST inhibitor and then were incubated with GSH and $Na_2S_2O_3$ in the same condition. Therefore, the probe can detect endogenous bisulfite in HepG2 cells.

By contrast, no obvious fluorescence change was observed in L-O2 cells pre-treated with RBC and GSH/ $Na_2S_2O_3$ in turn because of endogenous bisulfite was less in L-O2 cells (Fig. 6). This phenomenon indicates that the probe can distinguish between normal cells and cancer cells maybe on account of different TST content or activity, different membrane permeability of GSH or $Na_2S_2O_3$ for these two kinds of cells or other reasons. In order to further understand this verdict, exogenous bisulfite in L-O2 cells was investigated (Fig. 6). When L-O2 cells were cultured with the probe and different concentration of $NaHSO_3$, the ratio (blue/red) increased to nearly 10 times compared with the control group.

3.8 Practical application

Encouraged by the above results, some practical applications of this probe were explored. Bisulfite test strips were applied to monitor bisulfite content in water. As the HSO_3^- amount in the test strips gradually increased, the fluorescence color of the test strips changed from orange-red to blue under 365 nm UV light (Fig. 7). The attractive color changes of the experiments were
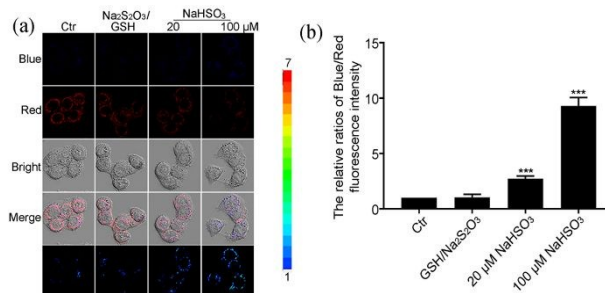
Fig. 6 (a) The fluorescent image of the L-O2 cells. The cells were incubated with RBC (1 µM) as control, and other reagents as test groups. (b) The ratio of fluorescence intensity (blue/red) of L-O2 cells incubated with probe RBC (1 µM) for 1 h and then with $NaHSO_3$ (0, 20, and 100 µM) for 1 h. The ratio images were all obtained as Fblue/Fred, λ_{ex} = 405 nm; λ_{em} = 450–610 nm (blue), λ_{em}= 640–700 nm (red). ***P < 0.01; (n = 3).
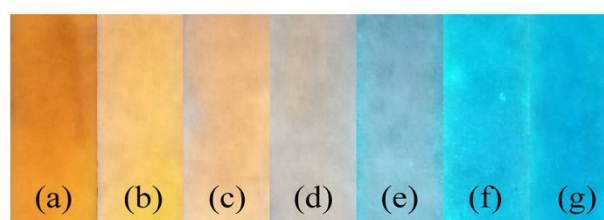
Fig. 7 Fluorescent changes of RBC (0.01 mg/mL)-coated test strips after soaked in different concentrations of HSO_3^- (a: 0, b: 1 equiv., c: 3 equiv., d: 5 equiv., e: 6 equiv., f: 7 equiv., g: 8 equiv.) aqueous solution.

ARTICLE

exactly same as that in solution (Fig. S16). The results showed that probe RBC could sensitively and simply detect bisulfite in practical samples with the naked eye.

Conclusions

In summary, a new ratiometric fluorescence probe constructed by coumarin and benzothiazole derivative based on FRTE mechanism was designed and synthesized. The probe (RBC) exhibited a significantly ratiometric, high selectivity and low detection limit. Importantly, the probe could rapidly respond to HSO_3^-/ SO_3^{2-} within 35 s. We anticipate that this sensing system should pave a new way for designing fluorescence ratiometric probe. Furthermore, RBC was mitochondria-targeted and was successfully used for fluorescence imaging of endogenous bisulfite in HepG2 with low cytotoxicity, which had a significantly assist to cancer diagnosis.

Conflicts of interest

There are no conflicts to declare.

Acknowledgements

Notes and references

1   K.K. Bertine and E. D. Goldberg, *Science*, 1993, **173**, 233–235.
2   W.Q. Chen, Q. Fang, D. L. Yang, H.Y. Zhang, X.Z. Song and J. Foley, *Anal. Chem.*, 2015, **87**, 609–616.
3   M.Y. Wu, K. Li, C.Y. Li, J.T. Hou and X.Q. Yu, *Chem. Commun.*, 2014, **50**, 183–185.
4   X. Dai, T. Zhang, Z.F. Du, X.J. Cao, M.Y. Chen, S.W. Hu, J.Y. Miao and B.X. Zhao, *Anal. Chim. Acta*, 2015, **888**, 138–145.
5   L. Tan, W.Y. Lin, S.S. Zhu, L. Yuan and K.B. Zheng, *Org. Biomol. Chem.*, 2014, **12**, 4637–4643.
6   D.P. Li, Z.Y. Wang, H.Su, J.Y. Miao and B.X. Zhao, *Chem. Commun.*, 2017, **53**, 577–580.
7   A. Isaac, C. Livingstone, A.J. Wain, R.G. Compton and J. Davis, *Trends Anal. Chem.*, 2006, **25**, 589–598.
8   C.M. Yu, M. Luo, F. Zeng and S.Z. Wu, *Anal. Methods*, 2012, **4**, 2638–2640.
9   V.S. Lin, W. Chen, M. Xian and C.J. Chang, *Chem. Soc. Rev.*, 2015, **44**, 4596–4618.
10 X. Wang, P. Li, Q. Ding, C.C. Wu, W. Zhang and B. Tang, *J. Am. Chem. Soc.*, 2019, **141**, 2061–2068.
11 Z.L. Wang, Y. Zhang, J. Song, Y.Q. Yang, X. Xu, M.X. Li, H.J. Xu and S.F. Wang, *Anal. Chim. Acta*, 2019, **1051**, 169–178.
12 H.D. Xiao, K. Xin, H.F. Dou, G. Yin, Y.W. Quan and R.Y. Wang, *Chem. Commun.*, 2015, **51**, 1442–1445.
13 L.W. He, X.L. Yang, Y. Liu, X.Q. Kong and W.Y. Lin, *Chem. Commun.*, 2016, **52**, 4029–4032.
14 Z.R. Lou, P. Li and K.L. Han, *Acc. Chem. Res.*, 2015, **48**, 1358–1368.
15 D. Srikun, E.W. Miller, D.W. Domaille and C.J. Chang, *J. Am. Chem. Soc.*, 2008, **130**, 4596–4597.
16 G. Chen, W. Zhou, C.Y. Zhao, Y.X. Liu, T. Chen, Y.L. Li and B. Tang, *Anal. Chem.*, 2018, **90**, 12442–12448.
17 S. Samanta, S. Halder, P. Dey, U. Manna, A. Ramesh and G. Das, *Analyst*, 2018, **143**, 250–257.
18 W.Y. Liu, D. Zhang, B.W. Ni, J. Li, H.B. Weng and Y. Ye, *Sens Actuators B Chem.*, 2019, **284**, 330–336.
19 M. Zhao, D.K. Liu, L. Zhou, B.Y. Wu, X.H. Tian, Q. Zhang, H.P. Zhou, J.X. Yang, J.Y. Wu and Y.P. Tian, *Sens Actuators B Chem.*, 2018, **255**, 1228–1237.
20 Y. Liu, J. Nie, J. Niu, W.S. Wang and W.Y. Lin, *J. Mater. Chem. B*, 2018, **6**, 1973–1983.
21 J. Li, Y. Gao, H.R. Guo, X.K. Li, H.Y. Tang, J. Li and Y. Guo, *Dyes Pigments*, 2019, **163**, 285–290.
22 Y. Liu, K. Li, M.Y. Wu, Y. H. Liu, Y.M. Xie and X.Q. Yu, *Chem. Commun.*, 2015, **51**, 10236–10239.
23 J.S. Lan, R.F. Zeng, Y. Ding, Y. Zhang, T. Zhang and T. Wu, *Sens Actuators B Chem.*, 2018, **268**, 328–337.
24 L.W. He, W.Y. Lin, Q.Y. Xu and H.P. Wei, *Chem. Commun.*, 2015, **51**, 1510–1513.
25 L. Yuan, F.P. Jin, Z.B. Zeng, C.B. Liu, S.L. Luo and J.S. Wu, *Chem. Sci.*, 2015, **6**, 2360–2365.
26 D.P. Li, Z.Y. Wang, X.J. Cao, J. Cui, X. Wang, H.Z. Cui, J.Y. Miao and B.X. Zhao, *Chem. Commun.*, 2016, **52**, 2760–2763.
27 J.J. Hu, N.K. Wong, Q.S. Gu, X.Y. Bai, S. Ye and D. Yang, *Org. Lett.*, 2014, **16**, 3544–3547.
28 P.C. Xue, P. Chen, J.H. Jia, Q.X. Xu, J.B. Sun, B.Q. Yao, Z.Q. Zhang and R. Lu, *Chem. Commun.*, 2014, **50**, 2569–2571.
29 M.Y. Wu, Y. Wang, Y.H. Liu and X.Q. Yu, *J. Mater. Chem. B*, 2018, **6**, 4232–4238.
30 L. Cui, Y. Zhong, W.P. Zhu, Y.F. Xu and X.H. Qian, *Chem. Commun.*, 2010, **46**, 7121–7123.
31 Y.H. Yan, H.L. Ma, J.Y. Miao, B.X. Zhao and Z.M. Lin, *Anal. Chim. Acta*, 2019, **1064**, 87–93.
32 A. Spadaro, M. Frotscher and R.W. Hartmann, *J. Med. Chem.*, 2012, **55**, 2469–2473.
33 B. Soni, M.S. Ranawat, R. Sharma, A. Bhandari and S. Sharma, *Eur. J. Med. Chem.*, 2010, **45**, 2938–2942.
34 K. Pudhom, K. Kasai, H. Terauchi, H. Inoue, M. Kaiser, R. Brun, M. Iharaa and K. Takasu, *Bioorg. Med. Chem.*, 2006, **14**, 8550–8563.
35 S. Bondock, W. Fadaly and M.A. Metwally, *Eur. J. Med. Chem.*, 2010, **45**, 3692–3701.
36 Q. Li, Y. Huang, T.Q. Chen, Y.B. Zhou, Q. Xu, S.F. Yin and L.B. Han, *Org. Lett.*, 2014, **16**, 3672–3675.
37 Y. Nagasawa, Y. Tachikawa, E. Yamaguchi, N. Tada, T. Miura and A. Itoh, *Adv. Synth. Catal.*, 2016, **358**, 178–182.
38 W.L. Wu, X. Zhao, L.L. Xi, M.F. Huang, W.H. Zeng, J.Y. Miao and B.X. Zhao, *Anal. Chim. Acta*, 2017, **950**, 178–183.
39 G.L. Song, A.K. Liu, H.L. Jiang, R.X. Ji, J. Dong and Y.Q. Ge, *Anal. Chim. Acta*, 2019, **1053**, 148–154.
40 L.B. Xu, X. He, Y.B. Huang, P.Y. Ma, Y.X. Jiang, X. Liu, S. Tao, Y. Sun, D.Q. Song and X.H. Wang, *J. Mater. Chem. B*, 2019, **7**, 1284–1291.